LiNaB4O7 Crystals as a Material for Optically Induced Elastoopticity

ARTICLE *in* CRYSTAL GROWTH & DESIGN · NOVEMBER 2006

Impact Factor: 4.89 · DOI: 10.1021/cg0602461

CRYSTAL GROWTH & DESIGN
2006
VOL. 6, NO. 12
2779−2782

$LiNaB_4O_7$ Crystals as a Material for Optically Induced Elastoopticity

I. V. Kityk,*,† A. Majchrowski,‡ J. Zmija,‡ Z. Mierczyk,§ and K. Nouneh⊥

Institute of Physics, AJD Czestochowa, Al. Armii Krajowej 13/15, Czestochowa, Poland, Institute of Applied Physics and Institute of Optoelectronics, Military University of Technology, 2 Kaliskiego Str., 00-908 Warszawa, Poland, and Laboratoire de Physique Appliquée et d'Automatique, Université de Perpignan, Perpignan, France

Received April 25, 2006; Revised Manuscript Received September 26, 2006

ABSTRACT: During bicolor optical treatment by Nd:YAG laser radiation ($\lambda = 1060$ nm) and its coherent second harmonic ($\lambda = 530$ nm) of the $LiNaB_4O_7$ (LNTB) crystals (space group *Fdd*2), a substantial increase in the elastooptic coefficient at $\lambda = 633$ nm (up to 9×10^{-13} m^2/N) was revealed. The corresponding effect was maximal for the diagonal piezooptic PO_{xxxx} tensor component, where *x* is directed along the second-order crystallographic axes. The effect appears at temperatures below 80 K and achieves its maximal value at $T = 4.2$ K. The phenomenon appears after 2 min of optical treatment under laser power densities above 0.6 GW/cm^2 and is saturated after 5 min of the bicolor optical coherent treatment. The elastooptical effect decreases at least one order at temperatures below 50 K and 6 min after switching off the bicolor laser treatment.

1 Introduction

In recent years, inorganic borate crystals have been extensively investigated in the search for new materials showing nonlinear optical (NLO) properties for applications in such areas as higher laser harmonics generation of laser radiation, parametrical optics, and self-frequency doubling lasers. Borates, because of their 3- or 4-fold coordination of boron atoms, in contrast to other inorganic materials, can form numerous anionic boron−oxygen groups, of which $B_3O_6^{3-}$, BO_3^{3-}, $B_3O_7^{5-}$, and BO_4^{5-} are of interest because of their electronic structures that lead to strong second-order NLO properties.[1] The borate anionic groups can react with different cations because of the specific properties of their band energy structure[2] that form as a result of quite complicated compounds. Among the most promising NLO borate crystals that have been discovered recently, the following should be mentioned: $CsLiB_6O_{10}$,[3] $Ca_4ReO(BO_3)_3$, Re═Gd, Y (ReCOB),[4,5] $K_2Al_2B_2O_7$,[6] BiB_3O_6,[7,8] $Ba_2Be_2B_2O_7$,[9] $BaAlBO_3F_2$,[10] and $La_2CaB_{10}O_{19}$.[11] Cheng et al.,[12] following the band structure approach, have shown that the borate crystals should be promising second-order NLO materials and that main efforts in crystal design should be directed toward appropriate borate cluster organization.

The crystals with the alkali cations, particularly Li ones, simultaneously show good parametrical NLO and acoustoelectronic properties.[13] The $LiNaB_4O_7$ (LNTB) crystals and their similarity to $Li_2B_4O_7$ suggest possible good parametric NLO properties, particularly mechanical ones.

So one can expect that by appropriately varying the cationic subsystem, one can create borate crystals with excellent optically induced acoustical and piezooptical properties. Following our previous band structure calculations,[14] we have found that space charge density noncentrosymmetry for the $KLiB_4O_7$ single crystals does not have sufficient polarizabilities to be optically induced despite an existence of the SHG effect.[15] One of the main reasons is the substantially different potentials for potassium and lithium. To achieve a sufficiently good photoinduced effect together with the piezooptical coefficients, the choice of cations should be a compromise. For example, $Li_2B_4O_7$ single crystals possessing good electromechanical properties are not too good for the optically induced effects. In parametric NLO effects, the phonon subsystem, which is very active for such kinds of crystals, begins to play a substantial role.[16] So one can guess that use of Li and Na may be a good compromise to achieve good photoinduced elastooptical effects. It is necessary to emphasize that for the case of lithium tetraborate, the existence of two lithium atoms substantially suppresses the photoinduced effects because of relatively low charge density space gradients.

In this work, we study LNTB single crystals with regard to a photoinduced piezooptic effect. Section 2 will be devoted to technology of the LNTB crystal growth and description of the photoinduced piezooptical setup. In Section 3, principal results of the photoinduced elastooptic will be given, together with the appropriate explanations.

2. Experimental Section

According to Keszler,[17] the $LiNaB_4O_7$ (LNTB) compound melts incongruently at 765 °C. Using the phase diagram for the binary system $Li_2B_4O_7$−$Na_2B_4O_7$, given by Keszler, we grew the LNTB single crystals by the top seeded solution growth (TSSG) method from solution containing 65 mol % $Na_2B_4O_7$ and 35 mol % $Li_2B_4O_7$. The approximate temperature of crystallization was 730 °C. A two-zone resistance furnace was used in LNTB crystal growth experiments that were carried out from a platinum crucible that was 40 mm in height and diameter. Eurotherm 2074 programmers controlled the temperature of the heating zones. The detailed description of the TSSG method and the equipment used can be found elsewhere.[18] The growing LNTB crystals were rotated at a rate of 5 rpm and very slowly pulled up at a rate of 1 mm/day. To get super-saturation, leading to crystallization of LNTB, we lowered the melt temperature at a rate of 0.05 K/h. The LNTB crystals showed strong anisotropy of growth velocities that resulted in a nonuniform growth, similar to the growth of polar BiB_3O_6 single crystals.[19] In some directions, growth was not observed at all, so the LNTB crystallization was strongly asymmetric around the seed rotation axis. The typical process took 10 days, and as-grown LNTB crystal dimensions were $1.0 \times 1.5 \times 1.5$ cm^3. They have orthorhombic space group $Fdd2$[18] ($a = 13.308(3)$ Å; $b = 14.098(2)$ Å; $c = 10.225(3)$ Å),[17] which is different from $KLiB_4O_7$.[20]

Figure 1 shows a principal setup for photoinduced elastooptic

* Corresponding author. E-mail: i.kityk@ajd.czest.pl.
† Institute of Physics, AJD Czestochowa.
‡ Institute of Applied Physics, Military University of Technology.
§ Institute of Optoelectronics, Military University of Technology.
⊥ Laboratoire de Physique Appliquée et d'Automatique, Université de Perpignan.

10.1021/cg0602461 CCC: $33.50
Published on Web 11/07/2006

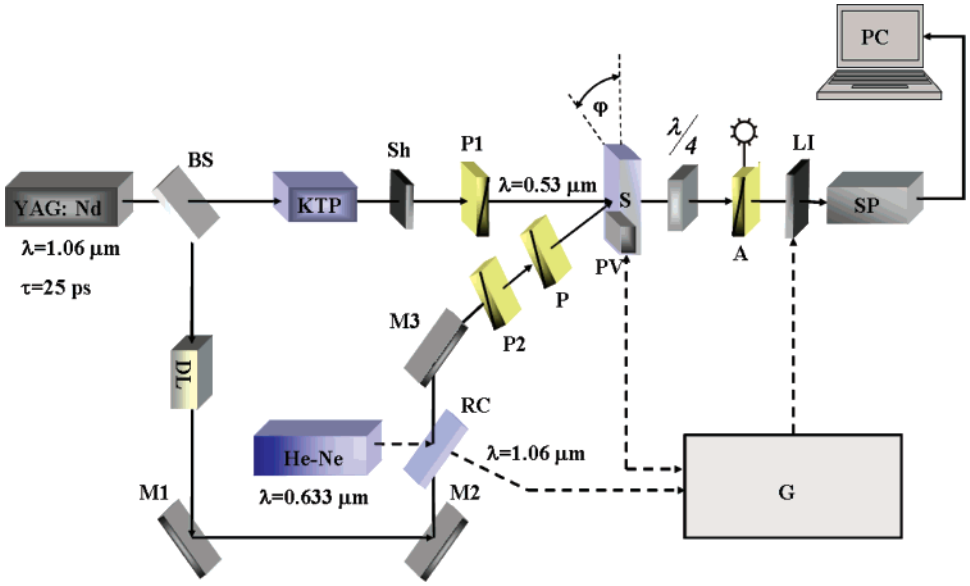

Figure 1. Principal experimental setup.

measurements. As a source of fundamental laser beam, a 25 ps pulsed Nd:YAG laser ($\lambda = 1.06\ \mu$m) with a peak power of about 1 MW was used. Using beam splitter **BS** and a system of the mirrors together with doubling frequency **KTP** crystal, we split the fundamental laser beam into two channels possessing beams with single and doubled frequencies. These two beams formed the grating typical for the disordered materials.[21] The delaying line **DL** retarded the probing polarized beam at 1.06 μm with respect to the 0.53 μm one to achieve maximal efficiency of the grating process. The delaying time was changed from 25 to 500 ps. Shutters **Sh** were used to close the particular channel and control the scattering background from the fundamental laser beam. Investigations of the elastooptic effect were done using the modified Senarmont method in the regime of the closed photoinducing beam (for several seconds). Static uniaxial mechanical stress was applied by a press vibrator (PV). Following this channel-probing beam method, we mounted the sample on a $\lambda/4$ plate and used an analyzer.

The output light intensity was detected using fast-response photomultipliers (PM) situated after the spectrophotometer (SP). The measurements were carried out in the single-pulse regime, with a pulse frequency repetition rate of 12 Hz and quasirectangular pulse duration varied within the 5−50 ps range at different applied electrostatic fields. The geometry of the experiment allowed us to measure the PO_{ijkl} tensor components. Such short-time kinetics allowed us to avoid specimen overheating. The pumping laser beam was scanned through the sample surface. The spectral selection of the pumping laser beams from probing and scattering light background was carried out by a grating **SP**. During evaluation of the time-delayed nonlinear optical response, we measured the angle of the rotation of the analyzer to achieve the minimum output light intensity. The He−Ne probing laser possessed a power of about 10 mW. Its beam was chopped by a mechanical press vibrator (PV) operated by an acoustic generator G used for measurements of the elastooptic constants. The measurements of the piezooptical (elastooptical) coefficient were done for the switched-off pumping beams.

The birefringence necessary for determination of the corresponding elastooptic coefficient from the Senarmont method was evaluated by an equation

$$\Delta n = \lambda \frac{\Delta\phi}{d} \qquad (1)$$

where $\Delta\phi$ is the angle of analyzer rotation necessary to reach the minimum of transparent light. The precision of birefringence Δn determination was equal to about 1×10^{-6}.

3. Results and Discussion

In Figure 2, the dependence of photoinduced changes for the diagonal piezooptical tensor component PO_{xxxx} is shown. The maximal changes were observed near liquid helium temperature (LHeT). One can see that between 3 and 4 min, the process demonstrated a jump for the diagonal piezooptical PO_{xxxx} tensor component, which, after 5 min of the phototreatment, was saturated at a level equal to about 8.2×10^{-13} m^2/N at $\lambda = 633$ nm. It is necessary to emphasize that for off-diagonal piezooptical coefficients, the corresponding values were 8 times smaller.

From Figure 3, one can see that the optimal ratio for achieving the maximal piezooptical coefficient corresponds to ratio fundamental (1060 nm)/seeding (530 nm) bicolor coherent beam power densities equal to about 32. The saturation process of the piezooptical coefficient begins at 0.56 GW/cm^2, which corresponds to inclusion to excitation of the anharmonic phonon modes. The results are presented at LHeT and for the angle between the incident pumping and writing beam equal to 28°. The photoinducing beam spots completely covered the He−Ne probing beams.

With the increase in the temperature at $T \approx 80$ K, we have a substantial diminishing of the effect (see Figure 4).

It is interesting to note that immediately after the photoinducing treatment was switched off, we observed a jump in the

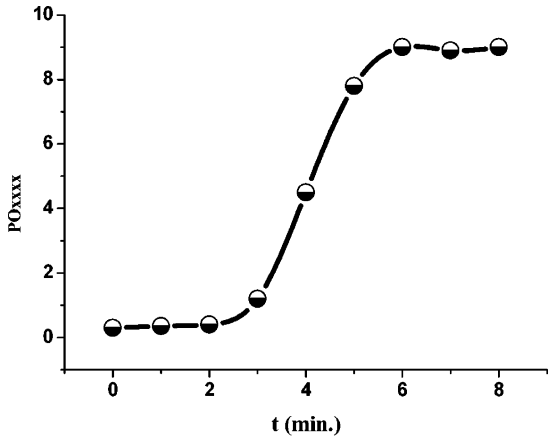

Figure 2. Dependence of the piezooptical coefficient versus photoinducing optical treatment for the pumping/writing beam's power density ratio equal to 32 at LHeT. The value of the piezooptical coefficient should be multiplied by 1×10^{-13} m^2/N. The average pump power density was equal to about 0.8 GW/cm^2.

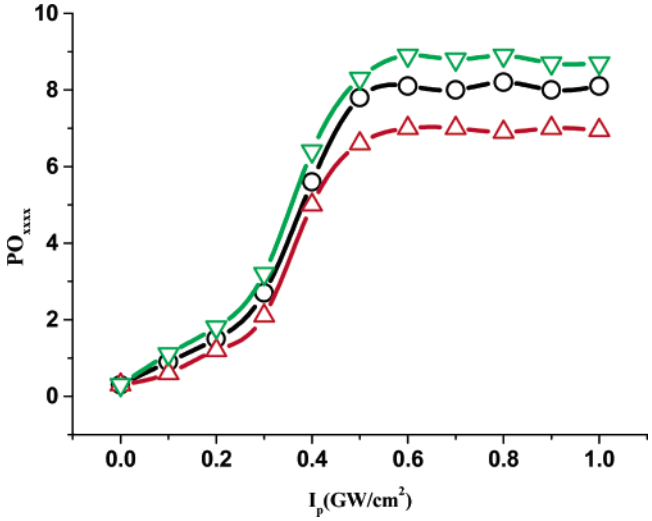

Figure 3. Dependences of the diagonal tensor piezooptical components versus the photoinducing pump power density for different ratio between the pumping and seeding (writing) beam power densities: inverted triangles, 32; rings, 50; triangles, 20. The results are presented for LHeT.

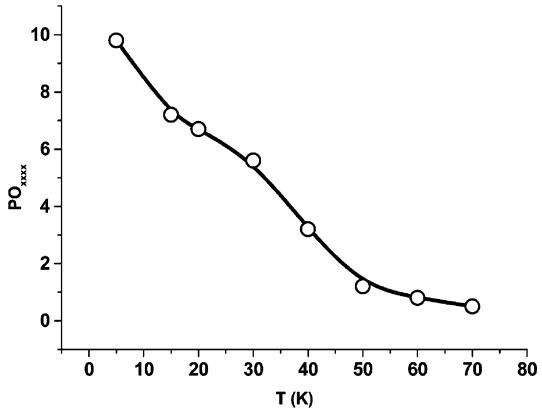

Figure 4. Temperature dependence of the piezooptical coefficient at pumping/writing beam power density ratio equal to 32.

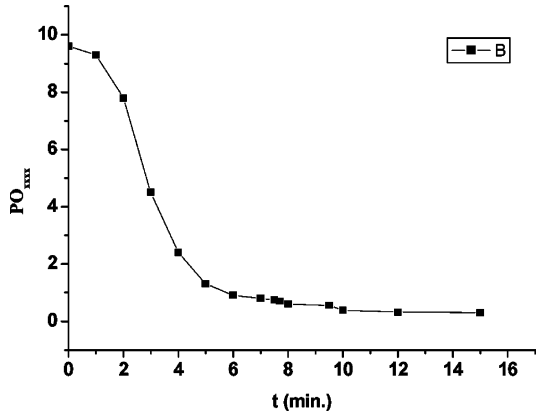

Figure 5. Time decay of the piezooptical coefficient for the same principal parameters.

PO_{xxxx} piezooptical coefficients (Figures 4 and 5), which probably reflects a drastic increase in the transition dipole moments of the crystal for the first moment of the interruption of the photophysical treatment, as was shown for the glasses.[21]

Such features may be explained within a framework of superionic conductivity existing for such kind of crystals. At low temperatures, it should be substantially smaller compared to the case when $T > 60$ K. As a consequence, the piezoelectric effect will be much larger; because of the photoinduced optically poled[21] mechanical stress, an enhanced piezooptical effect should form. Anisotropy of the crystals allows us to observe the maximal effect during the poling through the second-order axes.

Finally, in Figure 5, decay features of the diagonal piezooptical tensor components are observed to drop strongly during the first 4 min after the photoinducing lasers are switched off. The times are typical for the depopulation of the trapping levels occupied during the optical poling process.[21]

Conclusions

We have established that during photoinducing treatment by $\lambda = 1060$ nm and its doubled frequency 530 nm coherent beams of the $LiNaB_4O_7$ (LNTB) crystals, a substantial increase in the elastooptical (piezooptical) coefficient was revealed at $\lambda = 633$ nm (up to 9×10^{-13} m^2/N). The corresponding effect was maximal for the piezooptical PO_{xxxx} tensor component, where x was chosen to second-order crystallographic axes. The effect appears at temperatures below 80 K and achieves its maximal value at $T = 4.2$ K. The phenomenon appears during the 2 min of optical treatment under laser power densities above 0.6 GW/cm^2 and is saturated after 5 min bicolor coherent treatment. The elastooptical effect decreases at least one order at temperatures below 50 K and 6 min after switching off the bicolor laser treatment. The observed dependences are a consequence of specific mechanoelastic properties of the crystals and possible inclusion of the photo-operated dynamics of the trapping levels.

References

(1) Chen, C.; Lin, Z.; Wang, Z. *Appl. Phys. B* **2005**, *80*, 1.
(2) Maslyuk, V. V.; Islam, M. M.; Bredow, T. *Phys. Rev. B* **2005**, *72*, 125101−1.
(3) Tu, J. M.; Keszler, D. A. *Mater. Res. Bull.* **1995**, *30*, 209.
(4) Aka, G.; Khan-Harari, A.; Vivien, D.; Benitez, J. M.; Salin, F.; Godard, J. *Eur. J. Solid State Inorg. Chem.* **1996**, *33*, 727.
(5) Lukasiewicz, T.; Kityk, I. V.; Makowska-Janusik, M.; Majchrowski, A.; Galazka, Z.; Kaddouri, H.; Mierczyk, Z. *J. Cryst. Growth* **2002**, *641*, 237−239.
(6) Hu, Z. G.; Higashiyama, T.; Yoshimura, M.; Mori, Y.; Sasaki, T. *Z. Kristallogr.* **1999**, *214*, 433.
(7) Hellwig, H.; Liebertz, J. and Bohaty, L. *Solid State Commun.* **1999**, *109*, 249.
(8) Ghotbi, M.; Ebrahim-Zadeh, M.; Majchrowski, A.; Michalski, E.; Kityk, I. V. *Opt. Lett.* **2004**, *29*, 2530.
(9) Qi, H.; Chen, C. T. *Chem. Lett.* **2001**, *30*, 354.
(10) Hu, Z. G.; Yoshimura, M.; Maramatsu, K.; Mori, Y.; Sasaki, T. *Jpn. J. Appl. Phys.* **2002**, ***41***, L1131.
(11) Xu, X. W.; Chong, T. C.; Zhang, G. Y.; Cheng, S. D.; Li, M. H.; Phua, C. C. *J. Cryst. Growth* **2002**, *649*, 237−239.
(12) Cheng, W.-D.; Huang, J.-S.; Lu, J.-X. *Phys. Rev. B* **1998**, *57*, 1527−1533.
(13) Whatmore, R. W.; Shorrocks, N. M.; O'Hara, C.; Ainger, F. W.; Young, I. M. *Electron. Lett.* **1981**, *17* (1), 11.
(14) Smok, P.; Seinert, H.; Kityk, I. V.; Berdowski, J. *Mater. Lett.* **2003**, *57*, 4394.
(15) Adamiv, V. T.; Burak Ya, V.; Romanyuk, M. M.; Romanyuk, G. M.; Teslyuk, I. M. *Opt. Mater.* **2006**, doi:10.1016j:optmat2006.07.018.
(16) Elalaoui, E.; Maillard, A.; Fontana, M. D. *J. Phys.: Condens. Matter* **2005**, *17*, 7441.
(17) Maczka, M.; Waskowska, A.; Majchrowski, A.; Zmija, J.; Hanuza, J.; Peterson, G.; Keszler, D. *J. Solid State Chem.* **2006**, accepted for publication.

(18) Majchrowski, A.; Borowiec, M. T.; Michalski, E. *J. Cryst. Growth* **2004**, *264*, 201.
(19) Becker, P.; Liebertz, J.; Bohaty, L. *J. Cryst. Growth* **1999**, *203*, 149.
(20) Adamiv, V. T.; Burak, Ya, V.; Teslyuk, I. M. *J. Cryst. Growth* **2006**, *289*, 157.
(21) Balakirev, M. K.; Kityk, I. V.; Smirnov, V. A. Vostrikova, L. I.; Ebothe, J. *Phys. Rev. A* **2003**, *67*, 023806.

CG0602461